Expanded View Figures

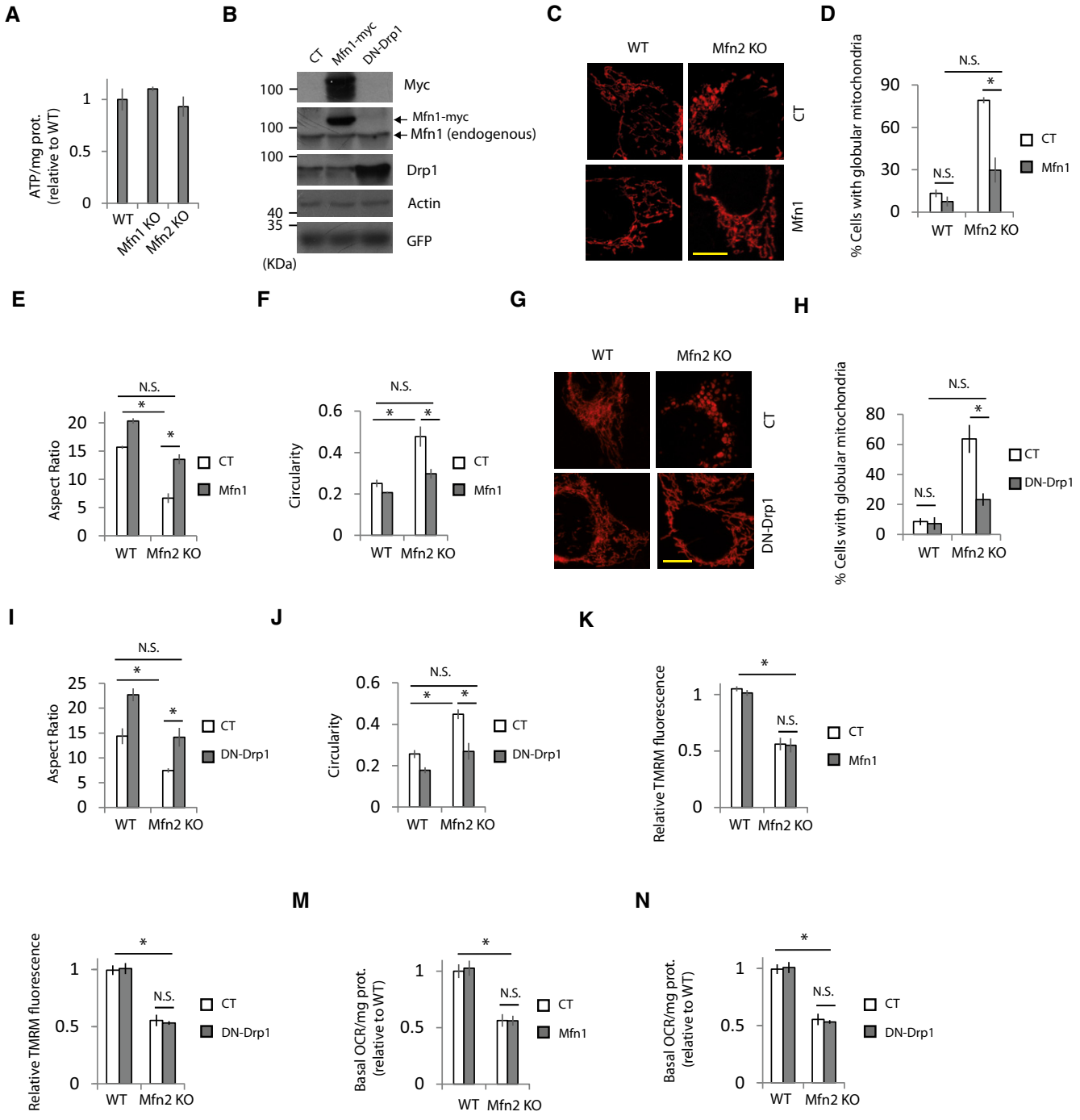

Figure EV1.

◀ **Figure EV1. Bioenergetics defects in Mfn2 KO cells are independent of mitochondrial morphology.**

A ATP levels in the indicated cell lines when metabolic flexibility is allowed ($n = 3$ independent experiments). Data are presented as mean ± SEM.

B Representative Western blots of the indicated proteins in Mfn2 KO fibroblasts transfected with plasmids expressing Mfn1, DN-Drp1, or a control plasmid (CT) ($n = 3$ independent experiments).

C–F Expression of Mfn1 restores mitochondrial morphology in Mfn2 KO MEFs. WT or Mfn2 KO MEFs were co-transfected with plasmids encoding mt-RFP and Mfn1 or control plasmids. (C) Representative images. Scale bar = 20 μm. (D) Percentage of cells displaying globular mitochondria ($n = 54$–414 cells analyzed in three independent experiments), (E) aspect ratio, and (F) circularity ($n = 260$–300 mitochondria analyzed in three independent experiments). Data are presented as mean ± SEM.

G–J Expression of DN-Drp1 restores mitochondrial morphology in Mfn2 KO MEFs. WT or Mfn2 KO MEFs were co-transfected with plasmids encoding mt-RFP and DN-Drp1 or control plasmids. (G) Representative images. Scale bar = 20 μm. (H) Percentage of cells displaying globular mitochondria ($n = 135$–470 cells analyzed in three independent experiments), (I) aspect ratio and (J) circularity ($n = 300$ mitochondria were analyzed in three independent experiments). Data are presented as mean ± SEM.

K, L Restoration of mitochondrial morphology by expression of (K) Mfn1 or (L) DN-Drp1 in Mfn2 KO MEFs has no effect on mitochondrial membrane potential ($n = 90$ cells analyzed in three independent experiments). Data are presented as mean ± SEM.

M, N Restoration of mitochondrial morphology by expression of (M) Mfn1 or (N) DN-Drp1 in Mfn2 KO MEFs has no effect on basal oxygen consumption rate ($n = 3$ independent experiments). Data are presented as mean ± SEM.

Data information: $^*P < 0.05$, one-way ANOVA followed by Tukey's post hoc test.

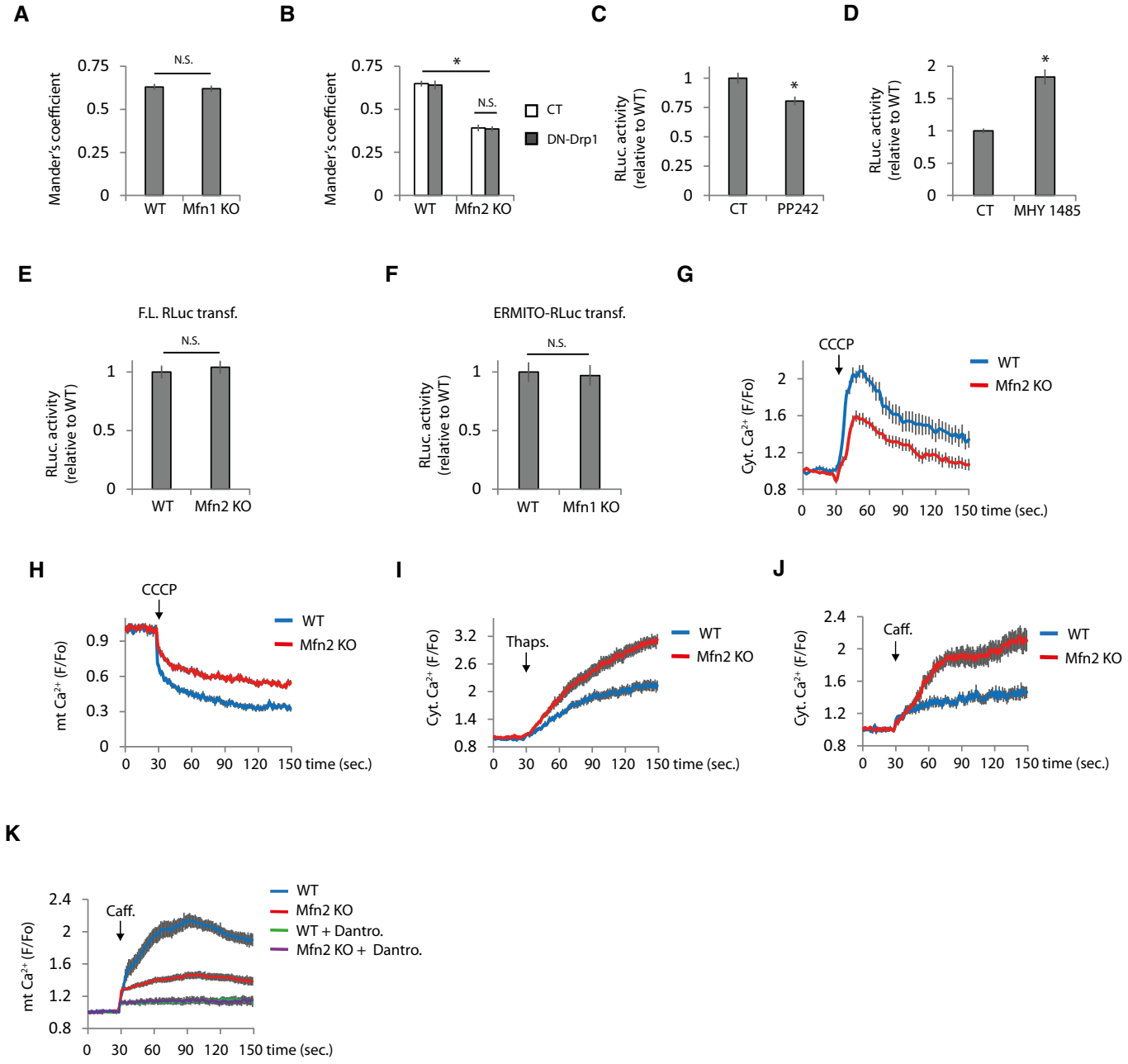

Figure EV2.

Figure EV2. ER and mitochondrial Ca^{2+} levels are deregulated in Mfn2 KO cells.

A Mander's coefficient of WT and Mfn1 KO cells co-transfected with plasmids encoding mitochondria-targeted RFP and ER-targeted GFP (n = 15 cells analyzed in three independent experiments). Data are presented as mean ± SEM.

B Restoration of mitochondrial morphology does not restores ER-mitochondria colocalization. Mander's coefficient of WT and Mfn2 KO cells co-transfected with plasmids encoding mitochondria-targeted RFP and ER-targeted GFP and the indicated plasmids (n = 15 cells analyzed in three independent experiments). Data are presented as mean ± SEM.

C, D ERMITO-Luc detects changes in ER-mitochondria contacts induced by manipulation of mTOR pathway. RLuc activity in cells transfected with ERMITO-Luc and treated with (C) the mTOR inhibitor PP242 (25 μM) (n = 4 independent experiments) or (D) the mTOR activator MHY 1485 (10 μM) (n = 6 independent experiments). Data are presented as mean ± SEM.

E There are not differences in the RLuc activity in the WT and Mfn2 KO cells transfected with plasmid expressing full-length Renilla Luciferase driven by the CMV promoter (n = 3 independent experiments). Data are presented as mean ± SEM.

F RLuc activity in WT and Mfn1 KO cells transfected with ERMITO-Luc (n = 3 independent experiments). Data are presented as mean ± SEM.

G, H Diminished Ca^{2+} levels in Mfn2 KO mitochondria. (G) Mitochondrial Ca^{2+} was released from mitochondria by applying CCCP (10 μM), and the rise in cytoplasmic Ca^{2+} was analyzed with Fluo-4 (n = 30 cells analyzed from three independent experiments). (H) Analysis of mitochondria Ca^{2+} levels in WT, and Mfn2 KO cells were transfected with the mitochondria-targeted Ca^{2+} sensor mt-Cepia (n = 30 cells from three independent experiments). Data are presented as mean ± SEM.

I Increased ER Ca^{2+} levels in Mfn2 KO cells analyzed by measuring cytoplasmic Ca^{2+} rise with Fluo-4 after thapsigargin (1 μM) treatment (n = 30 cells from three independent experiments). Data are presented as mean ± SEM.

J Caffeine induces higher ER Ca^{2+} release to the cytoplasm in Mfn2 KO cells. ER Ca^{2+} release was stimulated with caffeine (20 mM) as indicated, and cytoplasmic Ca^{2+} levels were analyzed with Fluo-4 (n = 30 cells from three independent experiments). Data are presented as mean ± SEM.

K The source of Ca2+ after caffeine treatment is from de ER. Inhibition of the RyR with dantrolene (10 μM) prevents caffeine-induced increase in mitochondrial Ca^{2+} levels (n = 30 cells from three independent experiments). Data are presented as mean ± SEM.

Data information: *P < 0.05, one-way ANOVA followed by Tukey's post hoc test.

Figure EV3. Restoration of bioenergetics defects in Mfn2 KO cells require proper Ca^{2+} transfer from the ER to mitochondria.

A, B ChiMERA is weakly expressed in MEFs. (A) Representative Western blots of the indicated proteins in Mfn2 KO fibroblasts transfected with RFP plus ChiMERA, GFP, or control (CT) plasmids as indicated (n = 3 independent experiments). Data are presented as mean ± SEM. (B) Representative confocal images of Mfn2 KO transfected cells with ChIMERA or GFP. Green fluorescent signal cannot be observed in ChIMERA expressing cells, although GFP molecule can be detected by three-step immunofluorescence using antibodies anti-GFP. Scale bar = 10 μm.

C MCU mRNA and protein levels were analyzed by qPCR and Western blot, respectively, of MEFs transfected with siRNA control (siCT) or a pool of 4 siRNAs targeting MCU (siMCU) (n = 3 independent experiments).

D MCU KD (siMCU) abolish mitochondrial Ca^{2+} uptake when the IP3R is stimulated with ATP (100 μM). WT and Mfn2 KO cells were transfected with siRNA control (siCT) or targeting MCU (siMCU). Mitochondrial Ca^{2+} uptake was analyzed. (n = 28–30 cells from three independent experiments). Data are presented as mean ± SEM.

E, F Inhibition of IP3R with (E) 2APB (50 μM) or (F) xestospongin C (XeC) (1.5 μM) prevents mitochondrial Ca^{2+} uptake caused by ATP treatment (n = 30 cells from three independent experiments). Data are presented as mean ± SEM.

G–I Treatment with 2APB or XeC prevents ChiMERA-mediated rescue of (G) MMP (n = 90 cells analyzed in three independent experiments), (H) ATP levels (n = 3 independent experiments), and (I) basal oxygen consumption rate (n = 3 independent experiments) in Mfn2 KO cells. Data are presented as mean ± SEM.

J, K 2APB or XeC treatment does not affect cell viability. WT and Mfn2 KO MEFs were treated with XeC (1.5 μM) or 2APB (50 μM) for 16 h, and then cell viability (J) was analyzed by fixing cells, DAPI staining and counting non-pyknotic nuclei as percentage of the total number of nuclei (n = 3 independent experiments). (K) Total number of nuclei per field was counted (n = 3 independent experiments). Data are presented as mean ± SEM.

L Mitochondrial mass is not affected by 2APB or XeC treatment. Representative Western blot of the indicated proteins of WT and Mfn2 KO MEFs treated for 16 h with XeC (1.5 μM), 2APB (50 μM) or vehicle (CT) (n = 3 independent experiments).

M Mfn2 KO show diminished expression levels of MCU but this is not rescued by ChiMERA expression. WT and Mfn2 KO cells were transfected with RFP and ChiMERA or control plasmid. After 24 h, the transfected cells were sorted and plated for another 24 h, when protein extracts were obtained. Representative Western blot of the indicated proteins (n = 3 independent experiments).

N Western blot with the indicated antibodies to characterize cultures of tamoxifen-inducible Mfn2 KO astrocyte cultures (n = 3 independent experiments).

O–Q Bioenergetic parameters were analyzed in WT and Mfn2 KO astrocytes transfected with ChiMERA or control plasmid. (O) MMP (n = 30 cells from three independent cultures). (P) Analysis of ATP levels after 6 h treatment with 2-DG (10 mM) (n = 3 independent experiments). (Q) Oxygen consumption rates. Proton leak was measured after application of oligomycin (1 μM), maximal after CCCP application (10 μM), and oligomycin (n = 5 independent experiments). Data are presented as mean ± SEM.

Data information: *P < 0.05, one-way ANOVA followed by Tukey's post hoc test except (C) that was used two-tailed Student's t-test.

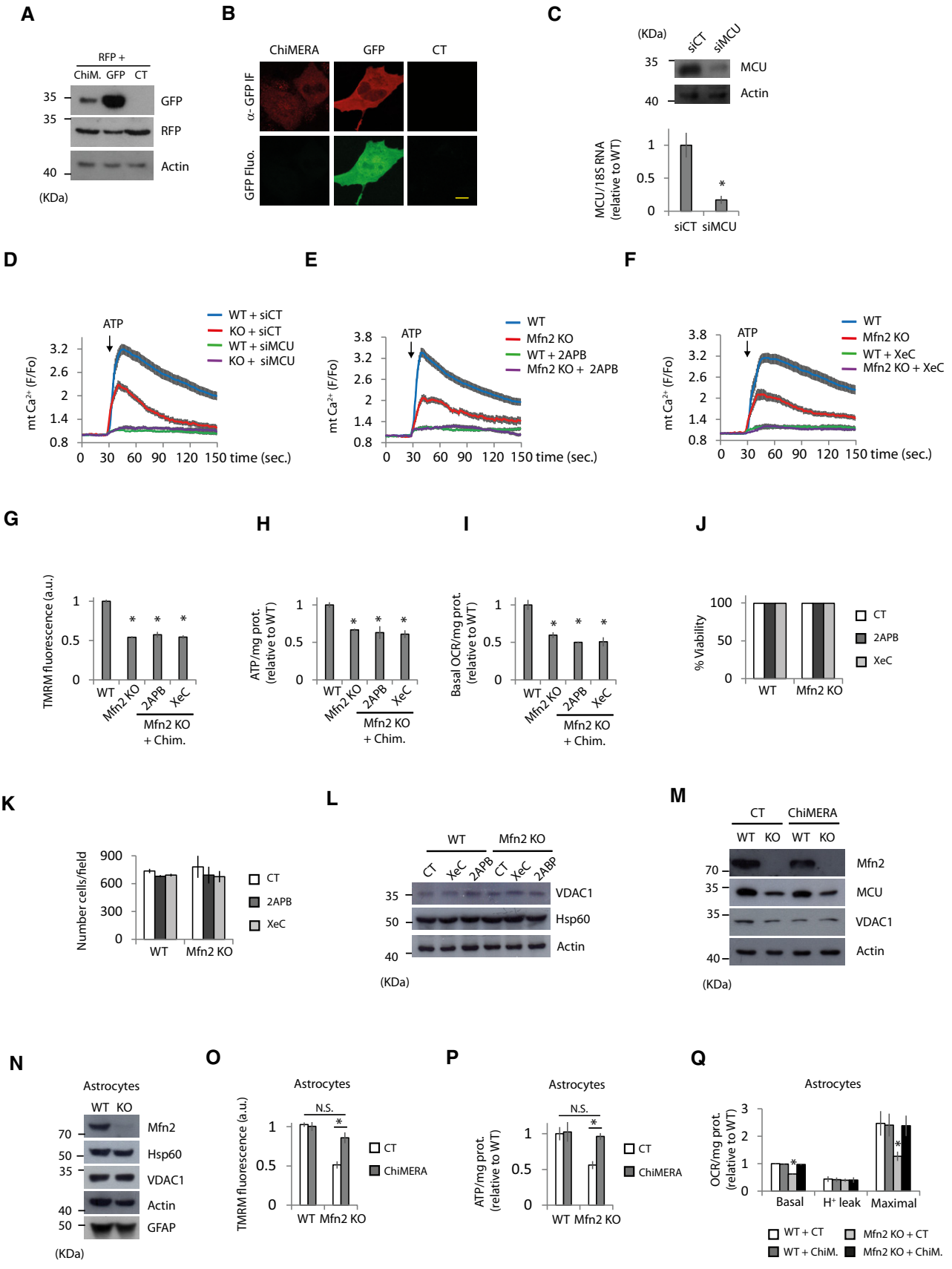
A
RFP +
ChiM. GFP CT
35
35
40
GFP
RFP
Actin
(KDa)
B
ChiMERA
GFP
CT
α- GFP IF
GFP Fluo.
C
(KDa)
siCT
siMCU
35
40
MCU
Actin
MCU/18S RNA (relative to WT)
1
0.5
0
*
siCT siMCU
D
ATP
WT + siCT
KO + siCT
WT + siMCU
KO + siMCU
mt Ca2+ (F/Fo)
3.2
2.6
2
1.4
0.8
0 30 60 90 120 150 time (sec.)
E
ATP
WT
Mfn2 KO
WT + 2APB
Mfn2 KO + 2APB
mt Ca2+ (F/Fo)
3.8
3.2
2.6
2
1.4
0.8
0 30 60 90 120 150 time (sec.)
F
ATP
WT
Mfn2 KO
WT + XeC
Mfn2 KO + XeC
mt Ca2+ (F/Fo)
3.8
3.2
2.6
2
1.4
0.8
0 30 60 90 120 150 time (sec.)
G
TMRM fluorescence (a.u.)
1
0.5
0
*
WT
Mfn2 KO
2APB
XeC
Mfn2 KO + Chim.
H
ATP/mg prot. (relative to WT)
1
0.5
0
*
WT
Mfn2 KO
2APB
XeC
Mfn2 KO + Chim.
I
Basal OCR/mg prot. (relative to WT)
1
0.5
0
*
WT
Mfn2 KO
2APB
XeC
Mfn2 KO + Chim.
J
% Viability
100
50
0
WT
Mfn2 KO
CT
2APB
XeC
K
Number cells/field
900
600
300
0
WT
Mfn2 KO
CT
2APB
XeC
L
WT
Mfn2 KO
CT
XeC
2APB
CT
XeC
2APB
35
50
40
VDAC1
Hsp60
Actin
(KDa)
M
CT
ChiMERA
WT KO WT KO
70
35
35
40
Mfn2
MCU
VDAC1
Actin
(KDa)
N
Astrocytes
WT KO
70
50
35
40
50
Mfn2
Hsp60
VDAC1
Actin
GFAP
(KDa)
O
Astrocytes
N.S.
*
TMRM fluorescence (a.u.)
1
0.5
0
WT Mfn2 KO
CT
ChiMERA
P
Astrocytes
N.S.
*
ATP/mg prot. (relative to WT)
1
0.5
0
WT Mfn2 KO
CT
ChiMERA
Q
Astrocytes
OCR/mg prot. (relative to WT)
3
2
1
0
*
*
Basal
H+ leak
Maximal
WT + CT
Mfn2 KO + CT
WT + ChiM.
Mfn2 KO + ChiM.

Figure EV3.

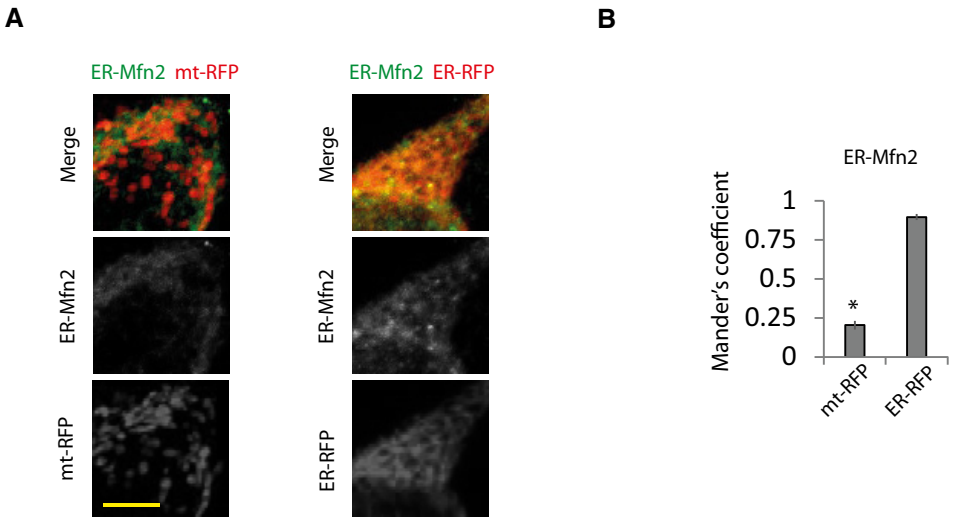

Figure EV4. ER-Mfn2 localizes in the ER.

A, B (A) Representative immunofluorescence imaging of Mfn1/2 DKO MEFs transfected with ER-Mfn2 and ER-RFP or mt-RFP and (B) colocalization of ER-Mfn2 with mitochondria or ER analyzed by Mander's coefficient (n = 10 cells analyzed in three independent experiments). Scale bar = 5 μm. Data are presented as mean ± SEM. *P < 0.05, two-tailed Student's t-test.

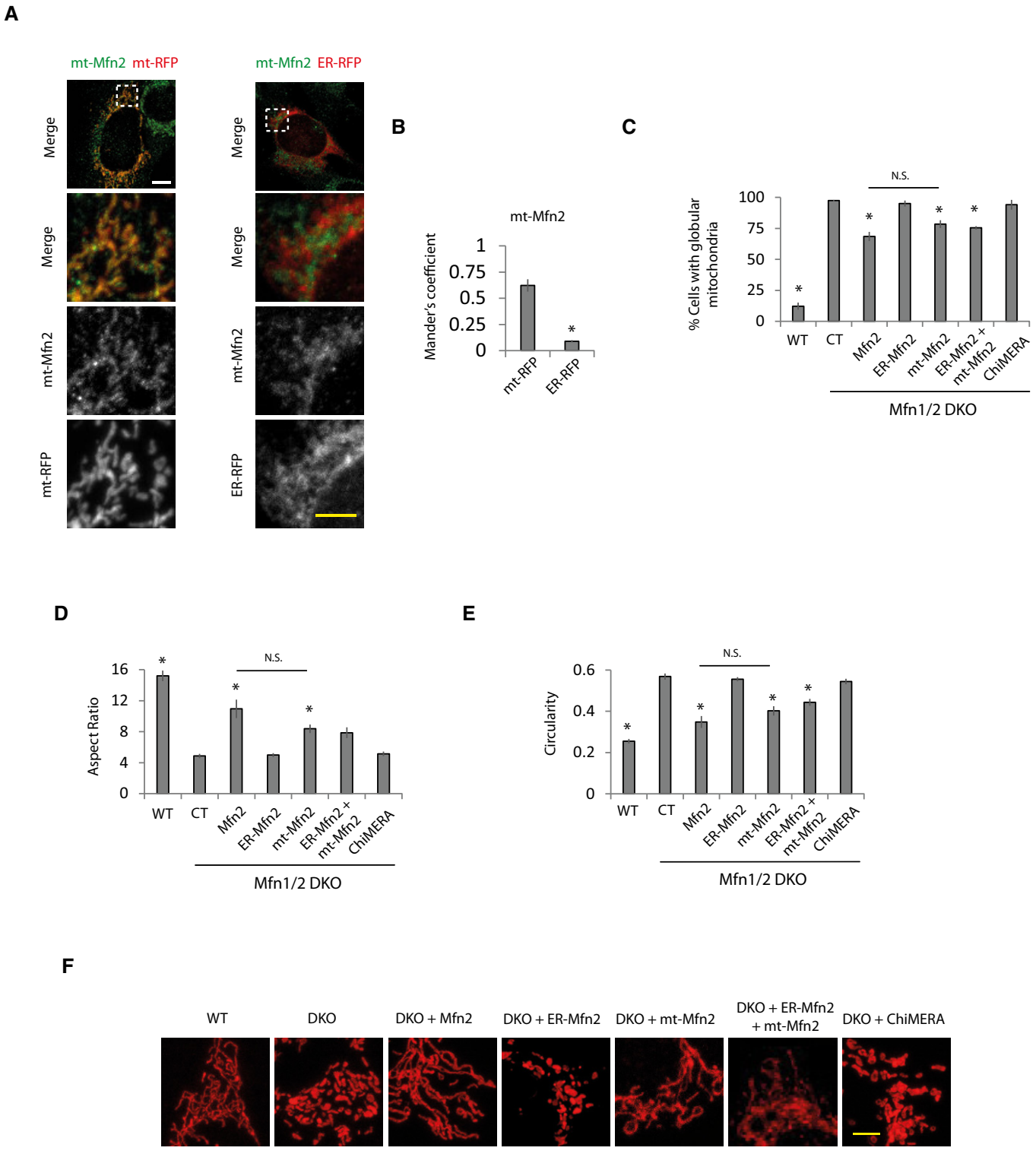
A
mt-Mfn2 mt-RFP
mt-Mfn2 ER-RFP
Merge
Merge
mt-Mfn2
mt-RFP
Merge
Merge
mt-Mfn2
ER-RFP
B
mt-Mfn2
Mander's coefficient
1
0.75
0.5
0.25
0
mt-RFP
ER-RFP
C
% Cells with globular mitochondria
100
75
50
25
0
N.S.
WT
CT
Mfn2
ER-Mfn2
mt-Mfn2
ER-Mfn2 + mt-Mfn2
ChiMERA
Mfn1/2 DKO
D
Aspect Ratio
16
12
8
4
0
N.S.
WT
CT
Mfn2
ER-Mfn2
mt-Mfn2
ER-Mfn2 + mt-Mfn2
ChiMERA
Mfn1/2 DKO
E
Circularity
0.6
0.4
0.2
0
N.S.
WT
CT
Mfn2
ER-Mfn2
mt-Mfn2
ER-Mfn2 + mt-Mfn2
ChiMERA
Mfn1/2 DKO
F
WT
DKO
DKO + Mfn2
DKO + ER-Mfn2
DKO + mt-Mfn2
DKO + ER-Mfn2 + mt-Mfn2
DKO + ChiMERA

Figure EV5.

Figure EV5. Mitochondria only targeted Mfn2 restores mitochondrial morphology to the same extent as Mfn2 in Mfn1/2 DKO cells.

A Representative immunofluorescence imaging of Mfn1/2 DKO MEFs transfected with mt-Mfn2 and ER-RFP or mt-RFP. Scale bar: 5 μm.

B Colocalization of mt-Mfn2 with mitochondria or ER analyzed by Mander's coefficient (n = 10 cells analyzed in three independent experiments). Data are presented as mean ± SEM. *P < 0.05, two-tailed Student's t-test.

C–F mt-Mfn2 expression restores mitochondrial morphology to the same extent as Mfn2 expression. Mfn1/2 DKO cells were transfected with control (CT), ChiMERA, or the indicated Mfn2 expression vectors and (C) percentage of cells displaying globular mitochondria (n = 310–668 cells analyzed in 3–6 independent experiments), (D) aspect ratio, and (E) circularity were calculated (n = 300 mitochondria analyzed from three independent experiments). Data are presented as mean ± SEM. (F) Representative images. White scale bar = 10 μm. Yellow scale bar = 5 μm.

Data information: *P < 0.05, one-way ANOVA followed by Tukey's post hoc test.

